Control Engineering: Maximizing Performance of the Fourth-Order Motion Setup

Tim Heiszwolf (XXXXX), Tessa Janssen (XXXXX), group 5

I. Introduction

A. The system

The goal of this paper is to identify, analyze, and design a controller for a fourth-order motion system aimed at maximizing performance. The system at hand consists of two rotating masses connected by a rod that acts as a spring, where one of the masses is driven by a DC-motor (further denoted as motor-side). The output of interest is the second mass (denoted as load-side) that is connected to an encoder, resulting in a non-collocated measurement. The system is shown in figure 1.

The open loop transfer function of the system H is given by the sum of the rigid body mode H_{rb} and the structural mode H_{st} where

$$H = H_{rb} \mp H_{st}, H_{rb} = \frac{1}{Ms^2}, H_{st} = \frac{1}{Ms^2 + ds + k} \quad (1)$$

where H_{st} is negative for the load side and positive for the motor side, M is the (equivalent to the) sum of both masses $(m_1 + m_2)$, d is the damping coefficient and k is (equivalent to the) spring constant.

B. Performance requirements

The the total required scanning stroke is 120 radians, with no more than 2.5 radians stroke for the turn-around of the masses (total allowed stroke of 125 rad). The set point for the system was therefore not predefined and was to be designed for the desired performance. The required performance of the system is defined in three regions that differ on the maximum allowed period of the total stroke trajectory, the maximum allowed Root mean Squared error (RMS), and the maximum allowed peak error. The error is only calculated during the constant velocity phase. The different regions are displayed in table 1. In addition the required robustness of the system is bounded by a modulus margin of at most 6 dB and the sampling rate can be no more than 4K Hz.

TABLE I: Performance regions criteria

Measure	Region I	Region II	Region III
Period T_r	10s $\leq T_r \leq$12s	10s $\leq T_r \leq$11s	$T_r <$10s
RMS	6 mrad	3 mrad	3 mrad
Max error	12 mrad	6.3 mrad	6.3 mrad

II. System Identification

A. Open loop FRF

To measure the setup it was chosen to perform an open loop FRF measurement. This approach was needed as the system itself, when closing the loop on the load-side was unstable. A measurement of the open loop was first needed to be able to design a simple stabilizing controller to continue with the next steps of optimization. A random Voltage noise signal with mean 0 and variance 0.3 was used as input to the plant and the measured output was the response of the system in radians on the load-side of the setup. This variance was chosen as a nicely middle in the range of allowed values (up to 0.5 max), this had good results and thus wasn't change, though theoretically higher could have been even better.

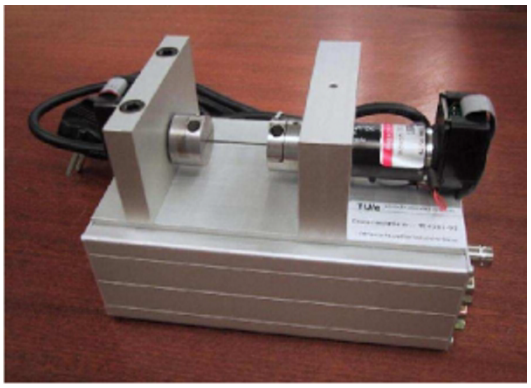

Fig. 1: Overview of the motion set-up.

The response was measured at a sampling rate of $f_s = 4000$ Hz, for a total duration of 120 seconds as this consistently provided smooth plots. Running the FRF for longer did not provide any additional information, so this duration was deemed enough. The Matlab script used to perform these measurements was written to cut out the first 5 seconds of sampling and run the measurements for an additional 5 seconds after, to account for disruptions in the measurement. The rotating masses would stagger briefly the moment the measurement was initiated, resulting in a discontinuity in the output. Cutting out these data points ensured an as clean as possible measurement of the system.

B. Determining the transfer function

To determine the transfer function of the plant, the Matlab function tfestimate.m was used. The input arguments for this function were defined as follows: $n_{fft} = 16000$, $noverlap = f_s/2$, and the window shape was the Hanning window. These parameters yielded a resolution of 0.25 Hz, which was sufficient to recognize the resonances that naturally occur in the plant. The resulting magnitude and phase plots are given in figure 2.

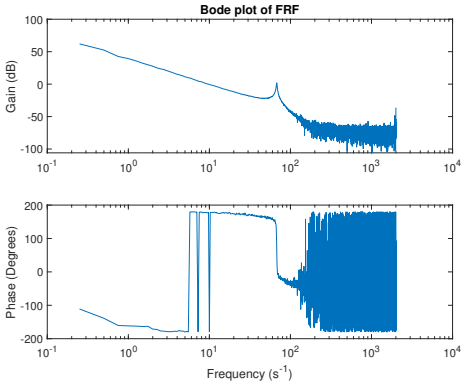

Fig. 2: Bode plot of the FRF measurement.

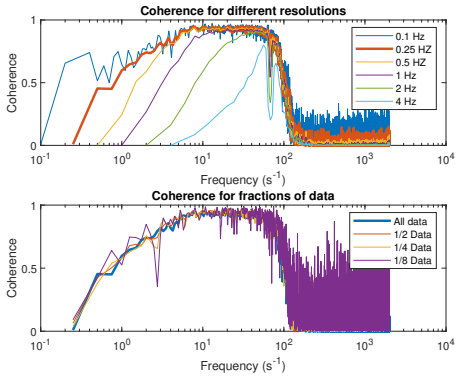

Fig. 3: Coherence plot of the FRF measurement.

C. Observations

The results of the FRF measurement are in line with what can be expected based on the modes of a two-mass, spring system where the measurement is non-collocated with the actuation. For lower frequencies the magnitude follows the mass-line (-2 slope) of the rigid body mode and the phase shows a corresponding -180 degrees lag. As expected there is one resonance around 60-70 Hz, which corresponds to the structural mode.

From a more physics based/intuitive perspective the behavior in gain is also to be expected. For low frequencies one expects the torsion bar to behave almost rigid and thus smoothly transfer any movement while for high frequencies the torsion bar barely has any time to transfer any movement to the load-side before it is twisted in the opposite direction. And the resonance of course would amplify the movement over multiple periods.

The highest measured frequency is indeed the Nyquist frequency at half the sampling rate at 2000 Hz. The lowest measured frequency is also indeed 0.25 Hz, which matches the intended resolution.

In figure 3 a coherence plot also can be seen, which can be used to check the quality of the FRF. Between 5 and 60 Hz the average coherence was around 0.91, which is is very good. But quickly dropped to zero afterwards between 80 and 110 Hz. This is to be expected since such high frequencies barely have any gain (less than -50 dB) and thus mostly noise and barely any signal was measured, which can also be seen the bode plot (figure 2). More data could likely not have improved this, as can be seen in the same figure, this could be argued since less data would shift the coherence drop to lower frequencies and that is not what is observed. Similarly, a different window size/resolution also wouldn't have helped. Interestingly the coherence around the resonance did get worse with a worse resolution, likely because those resolutions weren't able to properly resolve it.

Opposite of that, at lower frequencies the coherence also (more slowly) drops. As can be seen a larger window size could improve the result at lower frequencies. However it was chosen not to do this and keep the resolution at 0.25 Hz since it didn't significantly improve coherence at the lower frequencies which are interesting for control (1-10 Hz) but did introduce a lot of noise at higher frequencies.

TABLE II: Optimal reference parameters. First column is j_{max} (units rad/s^3), first result is a_{max} (rad/s^2), second result is v_{max} (units rad/s). Empty cells indicate impossible configurations.

Jerk	**Region 1**		**Region 2**		**Region 3**	
1380	216.21,	21.25				
1780	133.60,	21.42	282.658,	23.18		
2000	125.21,	21.45	180.31,	23.29		
2450	116.14,	21.50	152.82,	23.38	311.48,	25.77
3000	110.49,	21.53	140.30,	23.44	203.36,	25.93
4000	105.37,	21.57	130.43,	23.49	174.89,	26.04
5000	102.72,	21.59	125.726,	23.53	164.21,	26.09
∞	94.63,	21.66	112.53,	13.63	139.18,	26.25

D. Reference design

The reference can be seen as a piece-wise function: two constant velocity phases, two turn around phases consisting of two constant jerk phases and one constant acceleration phase. An example can be seen in figure 4.

To design this reference simple kinematics was combined with the requirements. This resulted in the possible configurations as seen in table II. It should be noted that other values are also possible but that those might not utilise the full allowed turn-around distance or the full allowed period, which is harder for the controller to track. However it might still be desirable to have such a reference which deviates from the optimal. For example to have more buffer in the turn-around to prevent overshoot due to error or to allow the system to recover from the turn-around before entering the constant velocity phase.

III. Controller design

A. Basic stabilizing controller

The first step after obtaining the FRF-measurement was to design a simple controller that would stabilize the system in closed loop. With this controller, it is possible to calculate the desired error measures and start optimizing performance. This first controller was designed by looking at the Nyquist plot corresponding to the FRF-measurement, which can be

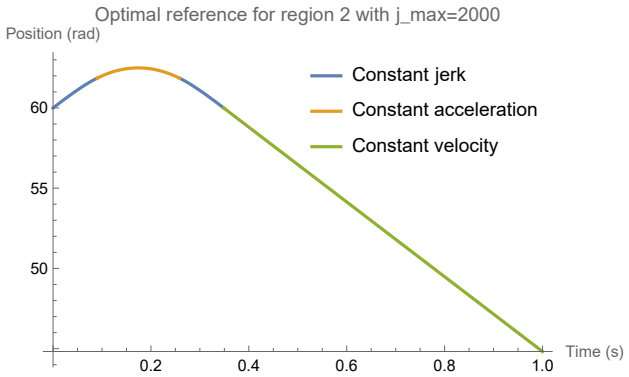

Fig. 4: The initial part of the optimal reference from table II for region 2 with $j_{max} = 2000$.

seen in figure 5a. From this plot it can be extrapolated that there is one encirclement of the the -1 point. In addition, the open loop transfer function as described in equation 1 contains no unstable poles. Applying this to the Nyquist criterion that states N = Z - P, where N is the amount of clockwise encirclements of the -1 points, Z the amount of unstable closed loop poles, and P the amount of unstable open loop poles, gives that there is one unstable closed loop pole, making the system unstable. To stabilize the system it is necessary to remove the clockwise encirclement in the Nyquist plot. To do this the first step was to add phase around the bandwidth frequency the make the Nyquist plot enter the unit disk in the third quadrant rather than in the fourth. This was implemented by adding a proportional-derivative controller in the form of

$$C_{PD} = P + \frac{P}{2\pi f_1} s \tag{2}$$

where f_1 = 5.3 Hz and P = 1. This exact value was found by trial and error to get to a point where the Nyquist contour enters in the third quadrant. It should be noted that the gain in the PD-controller was kept at a constant 1, as the actual gain of the full controller was changed with another component. On top of the phase lead, a notch filter was added to get rid of the resonance peak that is in this system at 68 Hz. This filter is defined as

$$C_{notch} = \frac{\frac{1}{2\pi f_2} s^2 + \frac{2\beta_1}{2\pi f_2} s + 1}{\frac{1}{2\pi f_3} s^2 + \frac{2\beta_2}{2\pi f_3} s + 1} \tag{3}$$

where f_2 = 68 Hz, β_1 = 0.005, f_3 = 70 Hz, and β_2 = 0.5. As there still was a lot of noise present in the higher frequencies, after the contour entered the unit disk, a first order low-pass filter was added of the form

$$C_{lowpass} = \frac{1}{\frac{1}{2\pi f_4} s + 1} \tag{4}$$

Where f_4 was set to 100 Hz. This value was determined by trial an error to make the controller stable and meet the robustness margins. As the nyquist contour kept being close to violating the margins, the gain of the system was lowered to 0.7. The Nyquist plot of the open loop including the stabilizing controller is shown in figure 5a.

TABLE III: Final controller components and parameters.

Filter	Parameters	Function
$Gain$	$P = 0.82$	Adjusted to meet robustness specs.
PD	$P = 1, D = 0.03$	Adding phase around 5 Hz to make the Nyquist contour enter in the third quadrant.
$Low-pass$	$f = 100Hz$	Filter out high frequency noise.
$Notch$	$zero: 68Hz$, $damping: 0.005$, pole: $70Hz$, $damping: 0.5$	Filter our the natural resonance of the system that occurs at 68 Hz.
$Notch$	$zero: 3.4Hz$, $damping: 0.055$, $pole: 3.6Hz$, $damping: 0.1$	Filter out the noise resulting from the constant velocity of the rotating mass.

B. Final controller design

The stabilizing controller as described in the previous section is not yet sufficient to achieve the desired performance. This also makes sense when looking at the coherence plots in figure 3. There appears to be quite some noise in the lower frequency region as the coherence is much lower than 1. This is also visible in the output of the system, there seems to be a constant oscillation around 3/4 Hz. On closer inspection, this disturbance is likely due to the constant velocity of the system which is set at 21 rad/s This indeed leads to a frequency of 3.4 Hz which approximately corresponds to the 3.52 Hz from the PSD plot in figure **??**. To counteract this frequency, an extra notch filter was added on the range 3.4-3.6 Hz, to dampen the response coming from here. In addition to this, the gain was increased as much a possible for the controller to still be within the specified margins (modulus margin $<$ 6 dB). The exact values of damping in the second notch and the gain were determined by trial and error of adjusting both controller until the desired result. An overview of the final controller is given in table 3.

IV. Feed-forward

A. Feed-forward

Due to the relatively low gain the error is still relatively high, to combat this feedforward was used. A reference consisting of 1/3rd acceleration, 1/3rd constant velocity and 1/3rd deceleration was made with a distance of 500 rad, maximum velocity of 250 rad/s and an acceleration of 250 rad/s^2 (which thus had a period of 6 seconds).

This tuning process can be seen in figure 7a. The first parameter to tune is K_{fc}, which represents the (velocity independent) coulomb friction, its goal is to equalize the tops of the acceleration/de-acceleration peaks. This was achieved with $k_{fc} = 0.004$. Next the goal was to tune k_{fv} which represents the dynamic friction, this was achieved by 'flattening' the error during acceleration and reducing error during constant velocity, and resulted in $k_{fv} = 0.0001$. Finally and most importantly K_{fa} is tuned to reduce the error during (de-)acceleration. It was tuned to $k_{fa} = 0.00365$. This

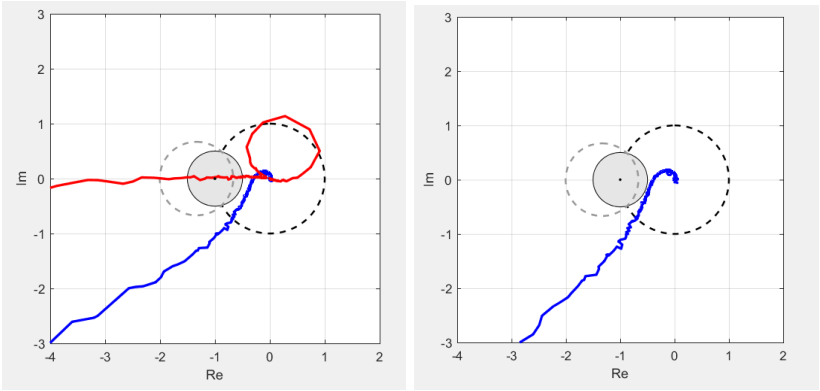

(a) Nyquist plot of the open loop FRF-measurement(red) and the stabilizing controller(blue). BW = 13.44 Hz, MM =4.20, PM = 47.6, GM = 10.4.

(b) Nyquist plot with the final controller design. BW = 16.71 Hz,MM = 5.30, PM = 46.3, GM = 8.2.

Fig. 5: Nyquist plots of the designed controllers.

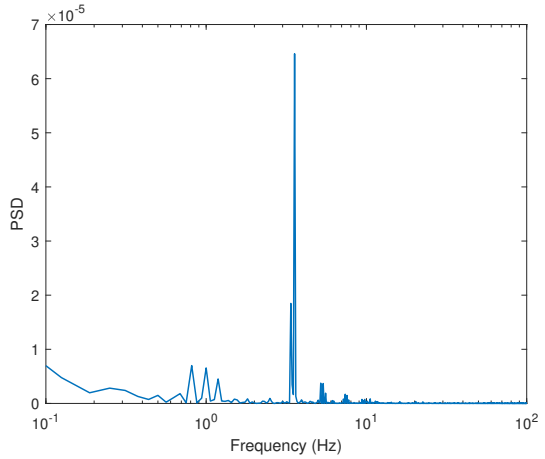

Fig. 6: The PSD error plot of the basic controller 1 in region 1.

feedforward controller 1 improved the performance from figure 7b to 7c in region 1.

While the result is a huge improvement it still is far from perfect. Thus a second feedforward controller was made which iterated on the first, specifically it was tuned on region 1 itself. The tuned parameters can be seen in table IV and the result in figure 7d.

B. Constant

As can be seen in figure 7d it can be seen that even with the best feedforward there still is an error but seemingly only in one direction. If one calculates the mean of the error it results in -1.4 mrad, this points towards a (small) steady-state error. It is likely caused by a asymmetry in the set-up itself since both the controller and feedforward are agnostic towards direction. This could be solved by adding an integrator to the controller however that is not something there currently is robustness margin left over for. So instead manually a constant is going to be added to the feedforward controller,

TABLE IV: Different configurations of feedforward controller.

	K_{fc}	K_{fv}	K_{fa}	Constant
Feedforward Controller 1	0.004	0.00001	0.00365	0
Feedforward Controller 2	0.004	0.00017	0.00046	0
Feedforward Controller 2.5	0.004	0.00017	0.00046	-0.001

this was determined to be -0.001 and was implemented in Feedforward controller 2.5 (FF2.5) and resulted in a new mean error of 0.2 mrad (see figure 8a). Since this was specifically tuned to region 1 it has the disadvantage that the feedforward controller would need to be returned for changes in reference, however that is not a big issue here since the references are quite similar, for example in region 2 the mean error with FF2.5 is -0.1 mrad. One possible approach for any future feedforward controller is to add 3 parameters similar to K_{fc}, K_{fv} and k_{fa} which are not depended on the direction of the velocity/acceleration but only the magnitude.

V. Experimental results

In the end a controller was designed (see chapter III-B) which performed quite well in combination with the feedforward tuning (using feedforward 2.5 as described in that section). In figure 8a the measurements are displayed using a reference to achieve performance region 1. the maximum error measured here is 9.7 mrad wit a mean RMS error of 3.4 mrad. This is well within the margins given for performance region 1.

Similar for a reference suitable for region 2 (see figure 8b), the maximum error is 7.5 mrad with a mean RMS of 3.2 mrad. Though slightly better than the performance in region 1, these values are not sufficient to pass the requirements. and thus region 2 was not achieved. It should also be noted that in region 2 one can see that the feed-forward is not properly

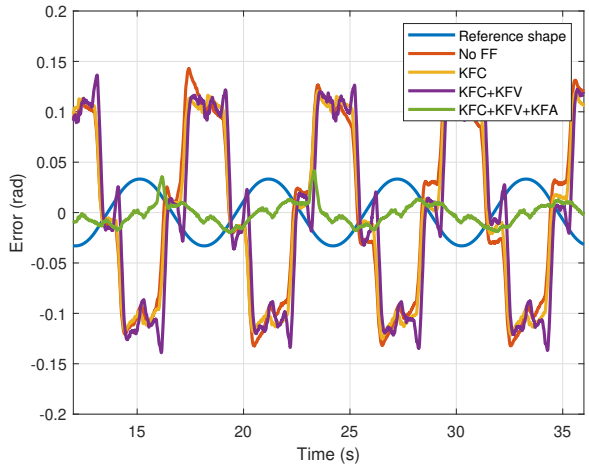

(a) Tuning of feedforward 1.

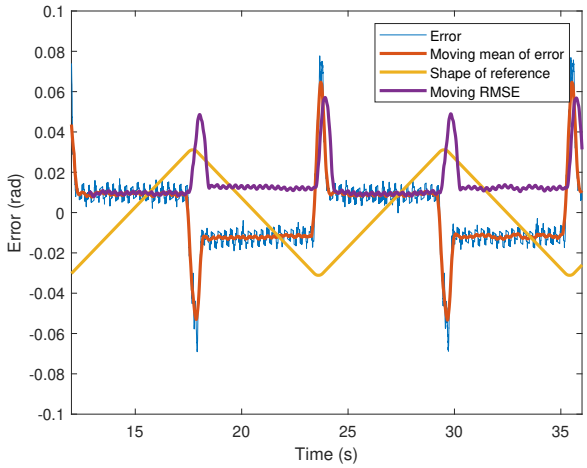

(b) Region 1 with controller 2 without feedforward.

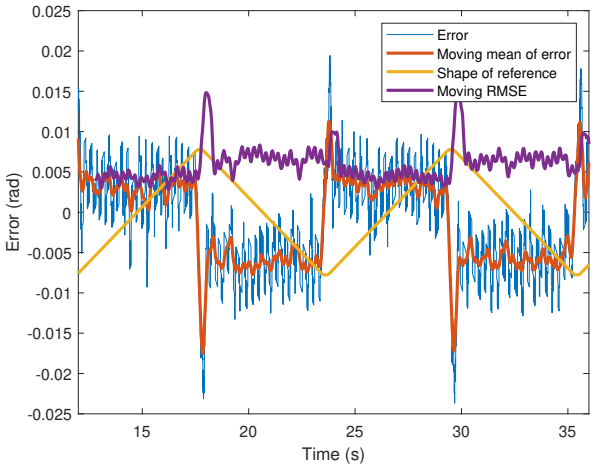

(c) Region 1 with controller 2 and feedforward 1.

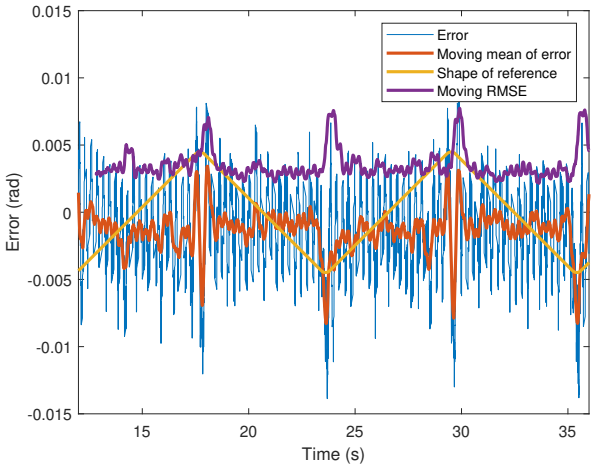

(d) Region 1 with controller 2 and feedforward 2.

Fig. 7: Feedforward tuning. Note the differing y-axis scales.

tuned since it can be seen that the k_{fv} is likely over-tuned since a over-correction in the error can be seen.

VI. Conclusions & Discussion

A. Conclusion

The goal of the paper was to investigate a fourth-order motion system and optimize performance as defined by three regions. After system identification, tuning of a feedback controller, and feedforward control, it was managed to satisfy both the RMS error and the maximum error needed for performance region 1. Though close, performance region 2 was not reached. Due to time constraints it was not possible to further extend the controller design to also satisfy the allowed errors for region 2 or region 3. The results show that by carefully looking at the source of errors in a system and using appropriate filters, one can tune a feedback controller to approach desired error margins.

TABLE V: Results of different controllers. RSME and max error are during the constant velocity period. Units are in miliradians.

	RMSE	**Max error**	**Margin turnaround**
Region 1 Controller 2	13.3	16.3	51.42
Region 1 controller 2+FF1	5.9	13.8	89.1
Region 1 controller 2+FF2	3.4	9.7	92.3
Region 1 controller 2+FF2.5	3.0	6.3	95.4
Region 2 Controller 2	12.1	16.2	51.42
Region 2 controller 2+FF1	5.6	12.2	92.2
Region 2 controller 2+FF2	3.6	8.1	101.7
Region 2 controller 2+FF2.5	3.2	7.5	95.4

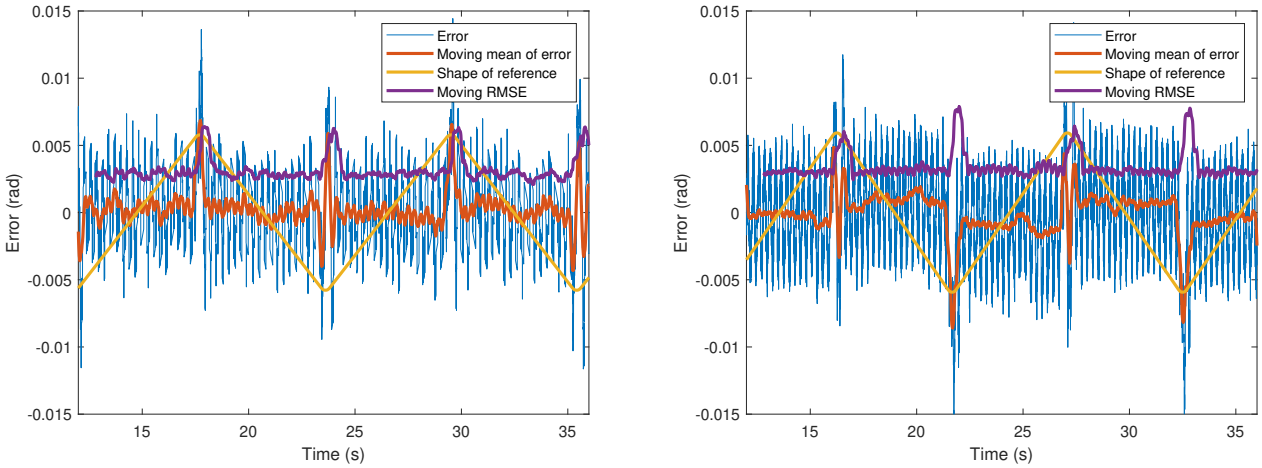

(a) Performance in region 1.

(b) Performance in region 2.

Fig. 8: Performance in two regions for controller 2 with the Feedforward controller 2.5.

B. Discussion

For further improvement two areas stand out. The largest being the large 3-4 Hz oscillations which still is present in the final controller. With further tuning and focus it might be possible to reduce it further or even eliminate it. While improving the controller one might also try and add a integrator to counteract some of the asymmetric behavior of the system (which here was inelegantly solved by adding a constant to the feed-forward controller). Finally the feed-forward could also be improved, the results of the original tuning was not that good and when it was further tuned on region 1 it resulted in a not very generalized result as can be seen in region 2.

EVENTUAL RESULT 6.5